J Med Syst (2017) 41: 31
DOI 10.1007/s10916-016-0675-2

A Multi Directional Perfect Reconstruction Filter Bank Designed with 2-D Eigenfilter Approach: Application to Ultrasound Speckle Reduction

Mukund B Nagare[1] · Bhushan D Patil[1] · Raghunath S Holambe[1]

Received: 15 September 2016 / Accepted: 7 December 2016 / Published online: 29 December 2016

Abstract B-Mode ultrasound images are degraded by inherent noise called Speckle, which creates a considerable impact on image quality. This noise reduces the accuracy of image analysis and interpretation. Therefore, reduction of speckle noise is an essential task which improves the accuracy of the clinical diagnostics. In this paper, a Multi-directional perfect-reconstruction (PR) filter bank is proposed based on 2-D eigenfilter approach. The proposed method used for the design of two-dimensional (2-D) two-channel linear-phase FIR perfect-reconstruction filter bank. In this method, the fan shaped, diamond shaped and checkerboard shaped filters are designed. The quadratic measure of the error function between the passband and stopband of the filter has been used an objective function. First, the low-pass analysis filter is designed and then the PR condition has been expressed as a set of linear constraints on the corresponding synthesis low-pass filter. Subsequently, the corresponding synthesis filter is designed using the eigenfilter design method with linear constraints. The newly designed 2-D filters are used in translation invariant pyramidal directional filter bank (TIPDFB) for reduction of speckle noise in ultrasound images. The proposed 2-D filters give better symmetry, regularity and frequency selectivity of the filters in comparison to existing design methods. The proposed method is validated on synthetic and real ultrasound data which ensures improvement in the quality of ultrasound images and efficiently suppresses the speckle noise compared to existing methods.

Keywords Filter banks · Perfect reconstruction · Ultrasound speckle reduction

This article is part of the Topical Collection on *Transactional Processing Systems*

✉ Mukund B Nagare
nagaremukund@gmail.com

Bhushan D Patil
bhushandpatil@gmail.com

Raghunath S Holambe
rsholambe@gmail.com

[1] S.G.G.S Institute of Engineering and Technology, Vishnupuri, Nanded, 431606, India

Introduction

In recent years, ultrasound imaging is widely used tool by a radiologist for medical diagnosis and treatment of various diseases. The ultrasound images are corrupted by speckle noise in its acquisition and transmission. This noise causes the poor image quality which is the major drawback of the ultrasound imaging. Speckle noise occurred in an ultrasound image by the constructive and destructive interferences from backscattered ultrasound waves. Speckle noise is modelled as the multiplicative noise. The noise appears in a granular pattern which makes it difficult to visually or automatically interpret the image data and reduces the efficacy of clinical diagnostics [1]. Therefore, speckle suppression is a critical preprocessing step and plays a vital role in ultrasound imaging. Speckle reduction improves the clinical diagnosis mainly in two applications: enhancement of edges and auto-segmentation improvements [1, 2]. Since the speckle noise diminishes the quality of ultrasound images, it is important to preserve the edges of relevant tissue information and textural information while removing the speckle. A number of algorithms have been proposed over a period to resolve the problem of speckle noise. Some of

the classical filters are the Lee filter [3], Frost filter [4], Kaun filter [5] and maximum a posteriori filter (MAP) [6]. However, these approaches do not assume any characteristics of the speckle and hence leads to remove important structural details of the tissues. Some of the improved methods attempted to overcome the problem of poor definition of edges such as speckle reducing anisotropic diffusion (SRAD) [7] and improved detail preserving anisotropic diffusion filter (DPAD) [8]. This method involves an edge sensitive anisotropic diffusion process. Similarly, advanced SRAD (OSRAD) [9] method has been proposed which uses the directional filtering using diffusion matrix to preserve the boundaries of the ultrasound image. However, these approaches still have the limitation of removing the structural details such as small lesions and small tissue structures of the tiny cyst. Recently, nonlocal means methods such as optimized Bayesian nonlocal means (OBNLM) [10] reported for speckle noise denoising, however, this method assumes a local region of homogeneity which may cause the enhancement of speckle noise in those regions. More recently proposed Anisotropic diffusion filter with memory based on the statistic of speckle content improved the denoising results, but, algorithms suffer from the computational burden. With the above facts, the problems in existing ultrasound image filtering approaches are summarized as: 1) the relevant structural information of the different tissues in the ultrasound image is not accurately characterized. 2) although the edges are preserved by diffusion approaches, diffusion filters suffers from over filtering which causes loss of information.

In consideration of these issues, this paper presents a novel Multi-Directional Perfect Reconstruction Filter bank based on 2-D eigenfilter approach. In this method, 2-D PR directional filters are designed with eigenfilter approach. The proposed method suppresses the speckle efficiently while preserving the structural tissue information of ultrasound image. This noise reduction occurs due to its multiscale multi directional decomposition scheme used with proposed 2-D directional filters.

In advanced medical computing and imaging devices, the two-dimensional (2-D) FIR filter banks (FBs) are widely used due to its important factor i.e. directionality. Directionality feature in transform efficiently handles the singularities present in 2-D signals. The 2-D FBs possess excellent phase characteristics and low coefficient sensitivity. Although 2-D filter bank designs are more complex as compared to 1-D FBs, it provides more flexibility in the design and gives better performance. The conventional mean max design approaches give the smallest length filters for a given specification [11]. In these algorithms, it is difficult to incorporate both time and frequency domain constraints. These algorithms require linear programming technique which demands large memory space and considerable time. However, proposed eigenfilter approach is based on the computation of an eigenvector of a appropriate real, symmetric, and positive definite matrix, which is numerically efficient [11]. Moreover the advantage of the eigenfilter approach is that we can add linear constraints easily and requires simple computation [12, 13]. In this method, the objective is to design 2-D filters by minimizing the error between desired frequency response and frequency response of the 2-D filter to be designed. Many design techniques have been developed for the design of 2-D filters in the literature [11, 14–18]. Some of these design techniques are based on window function methods, McClellan transformation methods and optimization techniques [15]. However, the limitation of these methods is that PR condition cannot be preserved for the resultant multidimensional filter bank [19].

Linear phase of the FBs is desirable in the medical image processing applications. To have a linear phase in 2-D FBs, the 2-D filter impulse response needs to be centrosymmetric [20]. This is obtained by using non-separable sampling in the filter bank called as quincunx subsampling. The quincunx subsampling in a 2-D two channel PR filter bank design is of particular importance. It results in the ideal subbands that are a diamond in shape. The Diamond shape filters preserve significant amount of horizontal and vertical information in the subbands, but it rejects most of the high diagonal frequencies. Human visual system is less sensitive to diagonal high spatial frequencies compared to horizontal and vertical high spatial frequencies. In such applications diamond shape filters are useful. However, fan-shaped filters with directional sensitivity are necessary in practice and have been used to process geoseismic data [21]. Various methods for the design of two channel quincunx filter bank have been presented in [22, 23]. Recently, design methods of 1-D and 2-D filter designs have been appeared in [12, 13, 24–27]. However, these methods are restricted on only diamond shaped 2-D filter designs. The 2-D wavelet based denoising for general images are proposed in [28, 29]. The bilateral filtering and stationary wavelet transform based approaches are found in the literature which is used for the ultrasound liver and mammography image denoising [30, 31]. There is no directional filter bank technique in the literature which is specifically used for medical images. However these directional filters are used for denoising of some medical images. These filters can be used for other imaging applications also.

In this paper, a Multi-Directional Perfect Reconstruction filter bank using Translation Invariant Pyramidal Directional Filter bank (TIPDFB) is proposed to reduce the speckle noise more effectively. The 2-D directional filters used in the TIPDFB [32] are designed by proposed eigenfilter approach which ensures the linear phase and perfect reconstruction properties of the filter bank. In this design,

we considered fan shaped, diamond shaped and checkerboard shaped filters which are important in the directional filter banks. We first design 2-D low-pass analysis filter by using eigenfilter formulation [27]. Then from the designed low-pass analysis filter, we impose linear constraints on the corresponding synthesis low-pass filter to achieve the perfect reconstruction condition and the corresponding synthesis low-pass filter is designed. The design ensures that the obtained filters satisfy the perfect reconstruction criteria and have better performance measures over existing 2-D filters. Moreover, the proposed denoising technique suppresses the speckle efficiently while preserving its directional information in the ultrasound images.

The paper is organized as follows. Section "Proposed method" provides a brief about proposed TIPDFB method and eigenfilter approach to the design of 2-D two channel linear phase perfect reconstruction FBs. The experimental results on ultrasound image denoising are discussed and compared in Section "Experimental results and discussion" with existing methods. The conclusion is given in Section "Conclusion".

Proposed method

To simplify the exposition, the architecture TIPDFB and its tree structure for directional filter bank implementation is discussed first. Then we discuss the proposed design method for 2-D directional filters using 2-D eigenfilter approach with few design examples.

Translation invariant pyramidal directional filter bank and its implementation structure

Directionality is an important factor in effective image representation. This is achieved by using directional filter banks which are unique in their ability to break down a multi-dimensional signal into directional subbands with higher angular resolution. The conventional 2-D DFB were first introduced by Bamberger and Smith in [33], which is implemented by l-level tree-structured decomposition which leads to 2^l subbands of wedge shape frequency partitioning as shown in Fig. 1a. This method has a disadvantage that low frequency band gets divided into all subbands. This paper uses the Translation invariant pyramidal directional filter bank (TIPDFB) which is also related to translation invariant contourlet transform. The key idea is to divide frequency plane into several parts which corresponds to specific frequency direction. This gives more accurate directional subbands with low-pass and high-pass frequency partitioning as shown in Fig. 1b. The low-pass subbands gives coarse approximation information whereas high pass subbands gives the directional information of the image. The proposed ultrasound image denoising architecture is shown in Fig. 2. The ultrasound speckle noise is modeled as a multiplicative noise [34]. This multiplicative noise is difficult to remove than the additive noise. The speckle noise model for an ultrasound image can be approximated as

$$g(x, y) = f(x, y)\eta_m(x, y) + \eta_a(x, y) \tag{1}$$

Where, $g(x, y)$ is the noisy recorded ultrasound image of spatial locations (x, y), $f(x, y)$ is the noise free image, $\eta_m(x, y)$ represent the multiplicative speckle noise and $\eta_a(x, y)$ is the additive noise. The effect of additive noise is insignificantly small compared with the multiplicative noise and hence it is discarded. Therefore above equation becomes

$$g(x, y) \approx f(x, y)\eta_m(x, y) \tag{2}$$

The logarithmic transformation is used before TIPDFB for converting multiplicative speckle noise into additive noise. This is defined as below.

$$\log g(x, y) = \log f(x, y) + \log \eta_m(x, y) \tag{3}$$

The TIPDFB is then applied on $\log g(x, y)$.

The TIPDFB transform mainly consists of two stages: a Laplacian Pyramid (LP) decomposition [35] and directional filter bank (DFB) decomposition [28] as shown in

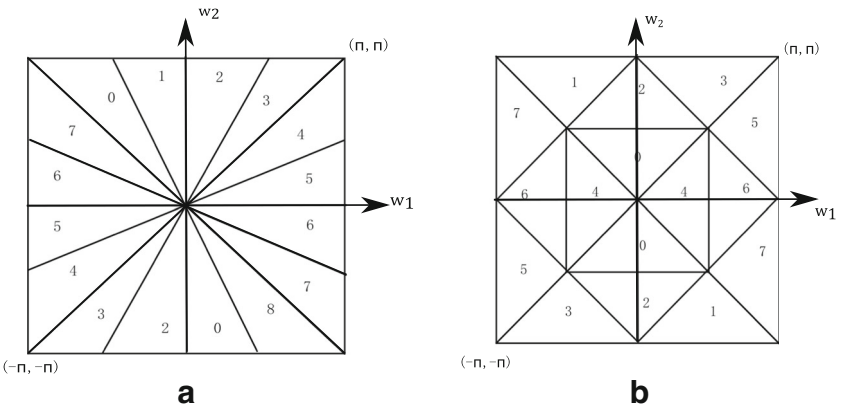

Fig. 1 Frequency Partitions (**a**) Bamberger and Smith's Method (**b**) Proposed TIPDFB

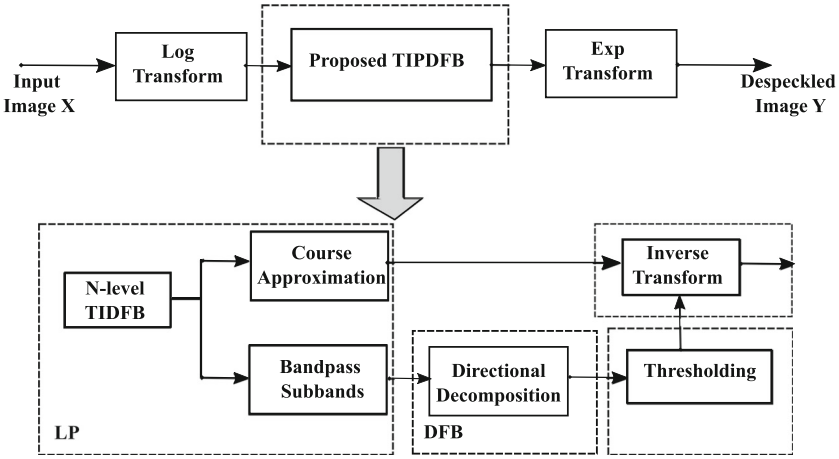

Fig. 2 General Structure for Speckle Reduction using TIPDFB

Fig. 2. Laplacian pyramid decomposes the ultrasound image into approximation information and radial bandpass subbands with different directional information. Then DFB is applied to each radial bandpass subbands where maximum fine structural details of the ultrasound image for a number of directions are extracted and preserved [28]. Speckle content is high frequency component due to which it lies in the high frequency subbands. Therefore all the directional subbands are thresholded with estimated threshold value to suppress the speckle noise. Translation invariant transform is necessary for image denoising application which avoids the errors sensitive to the positions of discontinuities in the image.

The DFB in second step can be implemented by using tree structure decomposition as shown in Fig. 3. This tree structure gives the frequency partitioning as shown in Fig. 1b. The 2-D two-channel PR directional filters used in this structure are designed by proposed 2-D eigenfilter approach given in next subsection. The PR property means that if there is no error in the filter bank, the reconstructed signal at the output is same as the input signal. Because the 2-D filters used at each stage of tree structure filter banks are PR filters and the entire filter bank is PR filter bank. The subband images of DFB are decimated by following sub-sampling matrices

$$Q_0 = \begin{bmatrix} 1 & -1 \\ 1 & 1 \end{bmatrix} \quad Q_1 = \begin{bmatrix} 1 & 1 \\ -1 & 1 \end{bmatrix} \quad R_0 = \begin{bmatrix} 1 & 1 \\ 0 & 1 \end{bmatrix}$$
$$R_1 = \begin{bmatrix} 1 & -1 \\ 0 & 1 \end{bmatrix} \quad R_2 = \begin{bmatrix} 1 & 0 \\ -1 & 1 \end{bmatrix} \quad R_3 = \begin{bmatrix} 1 & 0 \\ 1 & 1 \end{bmatrix} \tag{4}$$

After getting detail directional subbands, we apply hard thresholding to each subband and we reconstruct the thresholded subbands to achieve the speckle reduced denoised image. The optimal threshold value is estimated using Baye's shrinkage rule [36].

Fig. 3 Tree structure directional filterbank decomposition

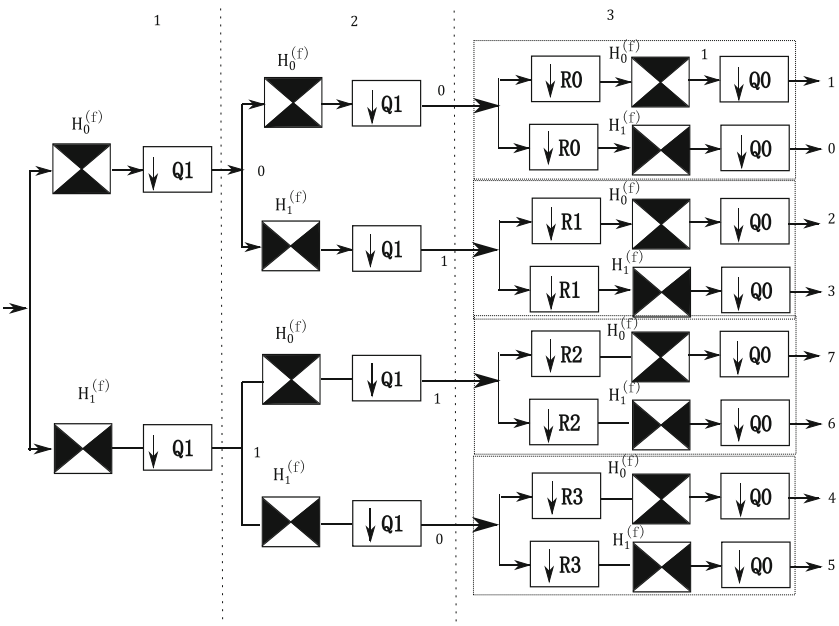

Background of 2-D two-channel linear phase FIR PR filter bank

A typical 2-D two channel PR filter bank with quincunx sampling is shown in Fig. 4.

The filters $H_0(z_1, z_2)$ and $H_1(z_1, z_2)$ represent the analysis low-pass and high-pass filters, respectively. Similarly, $F_0(z_1, z_2)$ and $F_1(z_1, z_2)$ denote synthesis filters. In the quincunx sampling, the points on $n_1 + n_2 =$ even quincunx sublattice are unmodified while points which are not on $n_1 + n_2 =$ odd sublattice are set to zero. That means, half of the samples are discarded effectively. The perfect reconstruction (PR) condition of the filter bank can be expressed as

$$H_0(z_1, z_2)F_0(z_1, z_2) - H_0(-z_1, -z_2)F_0(-z_1, -z_2) = 2z_1^{-l_1}z_2^{-l_2} \tag{5}$$

where l_1 and l_2 are delays.

$$H_0(z_1, z_2)F_0(z_1, z_2) - H_0(-z_1, -z_2)F_0(-z_1, -z_2) = 0 \tag{6}$$

If we choose high-pass filters as

$$F_0(z_1, z_2) = H_1(-z_1, -z_2) \quad \text{and}$$
$$F_1(z_1, z_2) = -H_0(-z_1, -z_2)$$

Equation 6 satisfies. Therefore from Eq. 5 product filter $P(z_1, z_2)$ can be defined as

$$P(z_1, z_2) = H_0(z_1, z_2)F_0(z_1, z_2) \tag{7}$$

which gives

$$P(z_1, z_2) - P(-z_1, -z_2) = 2z_1^{-l_1}z_2^{-l_2}. \tag{8}$$

Hence, the design objective of a PR filter bank can be problem of designing $P(z_1, z_2)$.

Eigen filter approach to design 2-D two-channel PR filter banks

Design of analysis 2-D lowpass filter

This section presents the eigenfilter approach to design of 2-D low-pass analysis filter. In this approach, objective is to minimize the quadratic measure of error function between the passband and stopband of the filter in 2-D frequency domain. This can be formulated as

$$E = \alpha E_p + \beta E_s \tag{9}$$

where

$$E_p = \iint_{passband} [H_D(w_1, w_2) - H_0(w_1, w_2)]^2 \, dw_1 dw_2$$

$$E_s = \iint_{stopband} [H_0(w_1, w_2)]^2 \, dw_1 dw_2.$$

where, $H_D(w_1, w_2)$ is the desired frequency response, $H_0(w_1, w_2)$ is the actual frequency response of 2-D filter and α, β are weighting constants which control the relative accuracies of the approximation in passband and stopband, respectively. Main focus is to minimise the error function which is written in the form of $E = \boldsymbol{a}^T \boldsymbol{J} \boldsymbol{a}$ where $\boldsymbol{a}$ is real vector and $\boldsymbol{J}$ is the real, symmetric and positive definite matrix. The intention is to find real vector **a** whose elements belongs to the 2-D filter impulse response $h_0[n_1, n_2]$.

Consider a quadrantal symmetric 2-D FIR filter with center of symmetry at origin

$$h_0[n_1, n_2], -N_1 < n_1 < N_1, \text{ and } N_2 < n_2 < N_2$$

The frequency response for quadrantal symmetric filter can be expressed as

$$H_0(w_1, w_2) = \sum_{n_1=0}^{\frac{N_1-1}{2}} \sum_{n_2=0}^{\frac{N_2-1}{2}} a(n_1, n_2) \cos(n_1 w_1) \cos(n_2 w_2) \tag{10}$$

where $H_0(w_1, w_2)$ is actual frequency response and $a(n1, n2)$ is related to filter impulse response $h_0[n_1, n_2]$ as below

$$\begin{aligned} a(0, 0) &= h_0[0, 0] && \text{for } n_1 = 0, n_2 = 0 \\ a(n_1, 0) &= 2h_0[n_1, 0] && \text{for } n1 = 1 : N_1 - 1 \\ a(0, n_2) &= 2h_0[0, n_2] && \text{for } n_2 = 1 : N_2 - 1 \\ a(n_1, n_2) &= 4h_0[n_1, n_2] && \text{for } n_1 = 1 : N_1 - 1, \; n_2 = 1 : N_2 - 1 \end{aligned} \tag{11}$$

Let, $N_1 = N_2 = N$ & Defining column vectors $\boldsymbol{a}$ and $\hat{\boldsymbol{c}}(w_1, w_2)$ as

$$\boldsymbol{a} = [a(0, 0), a(0, 1), \ldots, a(0, N_2) \mid a(1, 0), a(1, 1), \ldots, a(1, N_2) \mid \cdots \mid a(N_1, 0), a(N_1, 1), \ldots, a(N_1, N_2)]^T \tag{12}$$

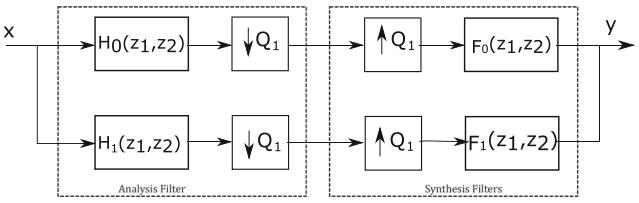

Fig. 4 Two channel filter bank with perfect reconstruction

$$\begin{aligned}\hat{\boldsymbol{c}}(w_1, w_2) = [&1, cos(w_2), \ldots, cos((N_2-1)w_2) \mid \\ &cos(w_1), cos(w_1).cos(w_2), \ldots, cos(w_1). \\ &cos((N_2-1)w_2) \mid \\ &cos((N_1-1)w_1, cos((N_1-1)w_1).cos(w_2), \ldots, \\ &cos((N_1-1)w_1)cos((N_2-1)w_2)]^T \end{aligned} \quad (13)$$

The frequency response for the filter $H_0(w_1, w_2)$ can be written as

$$H_0(w_1, w_2) = \boldsymbol{a}^T.\hat{\boldsymbol{c}}(w_1, w_2) \quad (14)$$

With this, the passband error and stopband error can be expressed as $E_p = \boldsymbol{a^T J_p a}$ and $E_s = \boldsymbol{a^T J_s a}$, with

$$\boldsymbol{J_p} = \iint_{passband} [\hat{\boldsymbol{c}}(\boldsymbol{\omega_{ref}}) - \hat{\boldsymbol{c}}(w_1, w_2)[\hat{\boldsymbol{c}}(\boldsymbol{\omega_{ref}}) - \hat{\boldsymbol{c}}(w_1, w_2)]^T dw_1 dw_2$$

and

$$\boldsymbol{J_s} = \iint_{stopband} [\hat{\boldsymbol{c}}(w_1, w_2)][\hat{\boldsymbol{c}}(w_1, w_2)]^T dw_1 dw_2$$

where $\boldsymbol{\omega_{ref}}$ is the reference frequency point in the passband region. Hence, the total error to be minimized in the Eq. 9 can be rewritten as

$$E = \alpha E_p + \beta E_s = \boldsymbol{a^T J a}, \text{ where } \boldsymbol{J} = \alpha \boldsymbol{J_p} + \beta \boldsymbol{J_s}. \quad (15)$$

Here, $\boldsymbol{J}$ is the real, symmetric and positive definite matrix. According to Rayleigh principle [37], the eigenvector corresponding to minimum eigenvalue of $\boldsymbol{J}$ gives minimum E. Therefore, the analysis low-pass filter coefficients obtained from the elements of the eigenvector corresponding to minimum eigenvalue of $\boldsymbol{J}$ yield minimum passband and stopband error.

Design of synthesis 2-D low pass filter

The coefficient of polynomial $H_0(z_1, z_2)$ are elements of eigenvector of J (as in Eq. 15) corresponding to minimum eigenvalue. We can obtain the coefficients of polynomial $F_0(z_1, z_2)$ using Eq. 8 and the coefficient of polynomial $P(z_1, z_2)$.

Assume that $h_0(n_1, n_2)$ and $f_0(n_1, n_2)$ are the zero phase filters with square region of support of the size $[P, Q]$, P & Q are the lengths of filter on n_1 & n_2 axes respectively. Hence $h_0(n_1, n_2)$ and $f_0(n_1, n_2)$ can be expressed as

$$\begin{aligned} h_0[n_1, n_2] &= \text{non-zero for } -P \le n_1, n_2 \le P \\ f_0[n_1, n_2] &= \text{non-zero for } Q \le n_1, n_2 \le Q. \end{aligned}$$

Note that, $p[n_1, n_2]$ is the 2-D convolution of $h_0[n_1, n_2]$ and $f_0[n_1, n_2]$ as given below

$$p[n_1, n_2] = \sum_{k_1=-Q}^{Q} \sum_{k_2=-Q}^{Q} f_0[k_1, k_2].(h_0[n_1 - k_1, n_2 - k_2]), \quad \text{for } -(P+Q) \le n_1, n_2 \le (P+Q). \quad (16)$$

Since $f_0[n_1, n_2]$ is zero phase, $f_0[n_1, n_2] = f_0[-n_1, -n_2]$. For zero phase filter with centro-symmetry the independent coefficients of $f_0[n_1, n_2]$ are

$$\begin{pmatrix} f_0[0, n_2], & 0 \le n_2 \le Q \\ f_0[n_1, n_2], & 1 \le n_1 \le Q,\ -Q \le n_2 \le Q \end{pmatrix}. \quad (17)$$

Hence, $f_0[n_1, n_2]$ has $2Q^2 + 2Q + 1$ number of independent coefficients. Therefore, Eq. 16 can be rewritten using independent coefficients of $f_0[n_1, n_2]$ as follows:

$$\begin{aligned} p[n_1, n_2] = \; & f_0[0, 0].h_0[n_1, n_2] \\ & + \sum_{k_2=1}^{Q} f_0[0, k_2].(h_0[n_1, n_2 - k_2] + h_0[n_1, n_2 + k_2]) \\ & + \sum_{k_1=1}^{Q} \sum_{k_2=-Q}^{Q} f_0[k_1, k_2]. \\ & \times (h_0[n_1 - k_1, n_2 - k_2] + h_0[n_1 + k_1, n_2 + k_2]) \\ & \text{for } -(P+Q) \le n_1, n_2 \le (P+Q). \end{aligned} \quad (18)$$

Note that, $h_0[n_1, n_2]$ and $f_0[n_1, n_2]$ are zero phase, which follows that $p_0[n_1, n_2]$ is also zero-phase (i.e. $p_0[n_1, n_2] = p_0[-n_1, -n_2]$) and set of independent coefficients are

$$\begin{pmatrix} \{n_1 = 0, & 0 \le n_2 \le N\} \\ 1 \le n_1 \le N, & N \le n_2 \le N \end{pmatrix}, \text{ where } N = P + Q. \quad (19)$$

From Eq. 5 for perfect reconstruction, it is required that

$$\begin{aligned} p[n_1, n_2] &= 1 \qquad \text{for } n_1 = n_2 = 0 \\ p[n_1, n_2] &= 0 \qquad \text{for } \begin{bmatrix} n_1 \\ n_2 \end{bmatrix} = Q_1 \begin{bmatrix} m_1 \\ m_2 \end{bmatrix} \\ & \qquad m_1, m_2 \text{ are integers and } n1, n2 \ne 0. \end{aligned} \quad (20)$$

This states that $p[n_1, n_2] = 0$ for all the points on quincunx sublattice: LAT(M)), i.e. for $n_1 + n_2 =$ even locations.

Let N_L denote the number of locations (n_1, n_2), where $p[n_1, n_2] = 0$. Then, we have

$$N_L = \frac{N-1}{2} + \left\lfloor \frac{N.(2N+1))}{2} \right\rfloor, \text{ when } N = \text{odd integer}$$

$$N_L = \frac{N}{2} + \frac{N.(2N+1)}{2}, \text{ when } N = \text{even integer}$$

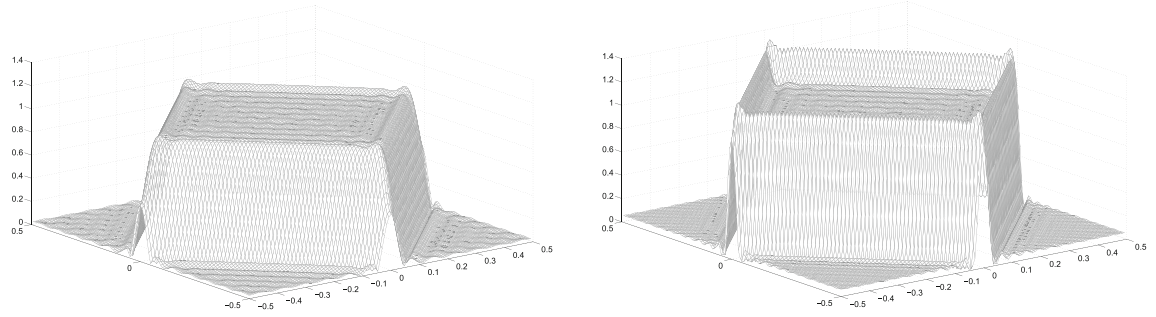

a $H_0(w_1, w_2)$ **b** $F_0(w_1, w_2)$

Fig. 5 Frequency responses of 2-D Diamond shaped FBs

Thus, from Eqs. 18 and 20, we can solve $N_L + 1$ equations for $2Q^2 + 2Q + 1$ unknowns, which are independent coefficients of $f_0[n_1, n_2]$.

Now, we impose linear constraints in the form of $\mathbf{Cf} = \mathbf{d}$ [12]. By arranging the independent coefficients $f_0[n_1, n_2]$ in vector $\mathbf{f}$, Eq. 20 can be rewritten as

$$\mathbf{Cf} = [1 \;\; 0 \;\; \cdots \;\; 0]^T. \tag{21}$$

Where $\mathbf{C}$ is matrix of size $(N_L + 1) \times (2Q^2 + 2Q + 1)$ which is obtained from Eq. 18, $\mathbf{f}$ is a vector of unknown coefficients of $f_0[n_1, n_2]$ of size $(2Q^2 + 2Q + 1) \times 1$ and $d = [1 \;\; 0 \;\; \cdots \;\; 0]^T$. Equation 21 has multiple solutions and we want one optimal solution. So, we rewrite constraints as follows

$$\hat{\boldsymbol{C}}\mathbf{f} = \mathbf{0} \tag{22}$$

where, the matrix $\hat{\mathbf{C}} = \mathbf{C} - \frac{\mathbf{d}.\hat{\boldsymbol{c}}^{\mathbf{t}}(\omega_0)}{H_D(\omega_0)}$ [12]. All the vectors which satisfy the constraints (22) can be expressed as $\mathbf{f} = \mathbf{Ub}$, where, the columns of $\mathbf{U}$ form an orthonormal basis for the null space of the matrix $\hat{\mathbf{C}}$ and $\mathbf{b}$ is any real vector of appropriate length. We used singular value decomposition (SVD) to find the orthonormal basis for the null space of matrix $\hat{\mathbf{C}}$. Our aim is to minimize $\mathbf{f^T Jf}$ under a constraint (22), which can be expressed as $\mathbf{E} = \mathbf{b^T U^T JUb}$. Hence, the optimal solution $\mathbf{b}$ of this simplified problem is the eigenvector of the matrix $\mathbf{U^T JU}$ corresponding to minimum eigenvalue. Finally, the desired optimal solution $\mathbf{f}$ is equal to $\mathbf{Ub}$ whose elements are the coefficients of the synthesis low-pass filter $f_0[n_1, n_2]$.

To design 2-D Diamond shaped analysis low-pass filter $h_0(n_1, n_2)$, we consider, w_{p1}, w_{p2} and w_{s1}, w_{s2} which describe the passband and stopband cutoff frequencies in the w_1 and w_2 axes. With filter size $N_1 = N_2 = 29$, $w_{p1} = w_{p2} = 0.4\pi$, w_{s1}=$w_{s1} = 0.6\pi$, $\alpha = \beta = 0.5$ and $\omega_{\mathbf{ref}} = (0, 0)$. For this $h_0(n_1, n_2)$, we design corresponding synthesis filter $f_0(n_1, n_2)$ with Q=35. The frequency response $H_0(w_1, w_2)$ and $F_0(w_1, w_2)$ are shown in Fig. 5a. and b. respectively.

Design of 2-D fan shaped FBs

The fan shaped filters can be obtained by transforming the rows of the diamond shape filters by $e^{-j\pi}$, that means the fan shaped FBs can be designed by interchanging the sign of the diamond shape FB in row or column direction. Hence,

$$H_0^f(w_1, w_2) = H_0(w_1 + \pi, w_2) \tag{23}$$

$$F_0^f(w_1, w_2) = F_0(w_1 + \pi, w_2) \tag{24}$$

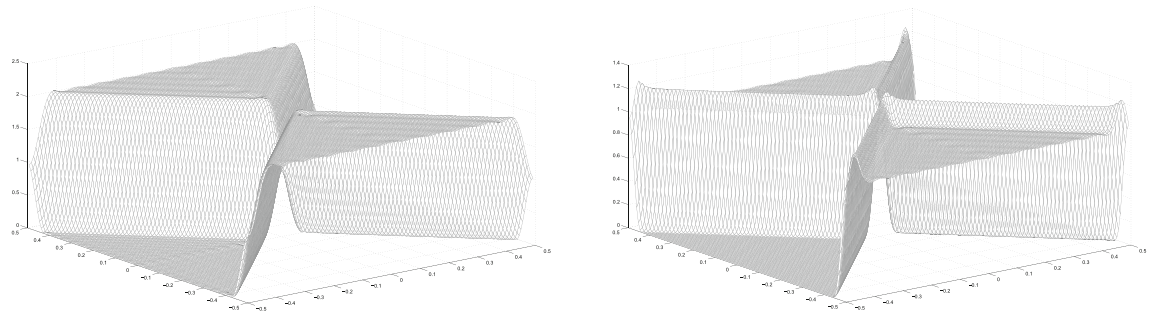

a $H_0^f(w_1, w_2)$ **b** $F_0^f(w_1, w_2)$

Fig. 6 Frequency responses of 2-D Fan shaped FBs

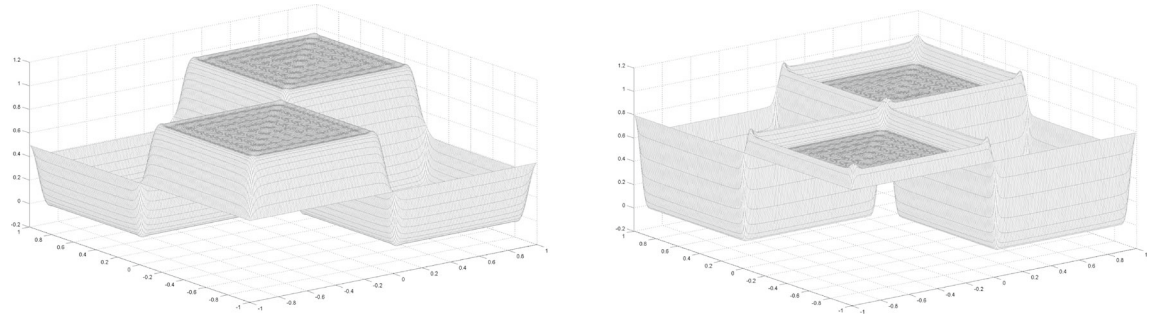

a $H_0^c(w_1, w_2)$ **b** $F_0^c(w_1, w_2)$

Fig. 7 Frequency responses of 2-D checkerboard shaped FBs

We design 2-D fan shaped analysis filter $h_0(n_1, n_2)$ in which w_s stopband cutoff frequency, with filter size $N_1 = N_2 = 23$, $w_s = 0.16\pi$, $\alpha = \beta = 0.5$. From designed low-pass analysis filter $h_0(n_1, n_2)$, we design corresponding synthesis low-pass filter $f_0(n_1, n_2)$ with Q=35. The frequency response $H_0^f(w_1, w_2)$ and $F_0^f(w_1, w_2)$ are shown in Fig. 6a and b respectively.

Where, $H_0^f(w_1, w_2)$ and $F_0^f(w_1, w_2)$ are analysis low-pass and synthesis low-pass filters of the Fan shaped filter banks respectively.

Design of 2-D checkerboard shaped FBs

Down-sampling of fan shape filters $H_0^f(w_1, w_2)$ and $F_0^f(w_1, w_2)$ by quincunx sampling matrix yields the checkerboard shaped filters.

$$H_0^c(z_1, z_2) = H_0^f(z_1 z_2, z_1 z_2^{-1}) \tag{25}$$

$$F_0^c(z_1, z_2) = F_0^f(z_1 z_2, z_1 z_2^{-1}) \tag{26}$$

For the design of checkerboard filters, we use the same specifications as fan shaped filters. The frequency response of analysis low-pass $H_0^c(w_1, w_2)$ and synthesis low-pass $F_0^c(w_1, w_2)$ filters are shown in Fig. 7a and b respectively.

Experimental results and discussion

To solve the issue of speckle noise in ultrasound image, the Multi-Directional Perfect Reconstruction (PR) Filter Banks have been proposed using 2-D eigenfilter design. We have computed following important properties of the designed 2-D filters and compared them with existing filters as below,

1. *Symmetry*: Symmetry can be used to measure the near-orthogonality of filters. In this paper, we use $\|H0 - F0\|^2$ as measure for symmetry.
2. *Regularity*: Regularity is one of the important properties of a wavelet FBs. The Regularity of the proposed filters can be computed by measuring the sobelov index. [37].
3. *Energy of the Error:* The Energy of error is also known as frequency selectivity. It is a measure of the energy of error between designed normalized 2-D low-pass filter and the ideal filter. Total energy of the error is defined as

$$E = \int_0^{2\pi} \int_0^{2\pi} | D(w_1, w_2) - H(w_1, w_2) |^2 \, dw_1 dw_2$$

The results have been presented in Table 1. It is observed that the proposed 2-D filters designed by 2-D eigenfilter method provide better symmetry, good regularity and lower energy of the error which leads to the better frequency

Table 1 Properties measure of the proposed 2-D filters

Type of filter	Method	Energy of the error	Symmetry	Regularity
Diamond (29x29)	Eslami's Method [38]	1.3434e+06	1.1062	0.0814
	Yue Lu Method [29]	3.0497e+05	1.5931	0.0055
	Proposed method	6.2447e+04	0.1110	0.1180
Fan (23x23)	Eslami's Method [38]	10.0611e+05	1.1062	0.0608
	THFB [39]	1.3434e+06	1.5931	−0.18616
	Proposed method	4.6191e+04	0.1595	0.06107
Checkerboard (23x23)	Eslami's Method [38]	2.4596e+05	0.89462	0.05185
	THFB [39]	8.3711e+06	1.53469	−0.19078
	Proposed Method	1.5401e+05	0.15007	0.06611

selectivity of the filters as compared to other design methods and hence gives better result in denoising of speckled images. These filters are then used in a multi-directional perfect reconstruction filter bank. In the proposed approach, TIPDFB separates directional information of the ultrasound image which is relevant to the clinical features into different directional subbands. Noise generally contained in the detail subbands, therefore, we threshold the detail subbands to suppress the speckle content present and reconstruct the original image. We obtained hard thresholding using Bayes' shrinkage rule. This threshold is capable of preserving structural information of the ultrasound image.

To evaluate the performance of proposed method, we performed several experiments on synthetic images and real ultrasound images. The performance of the proposed method is compared with existing speckle reduction methods such as SRAD [7], OBNLM [10], and ADMSS [40]. Figure 8a shows a synthetic image of kidney phantom in

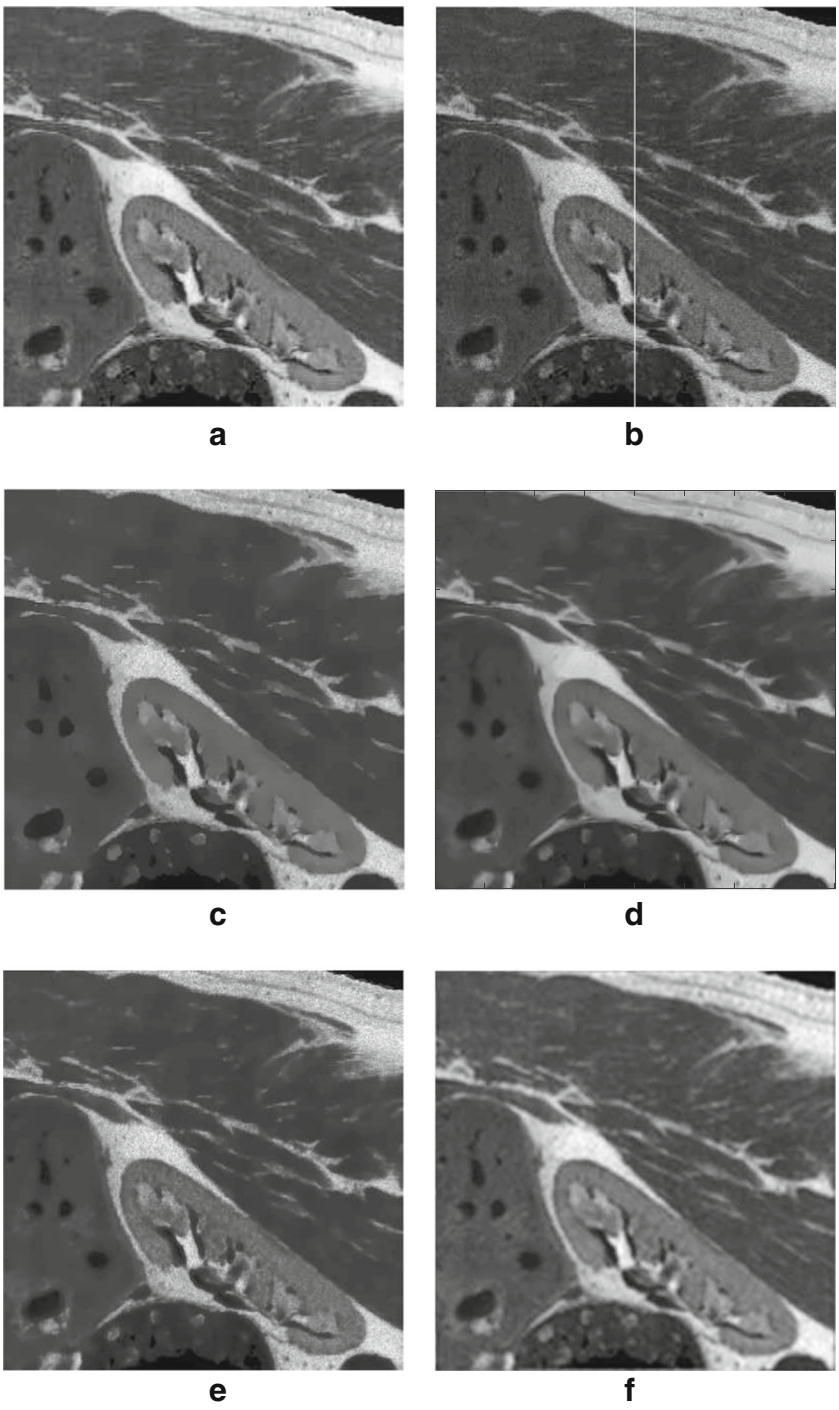

Fig. 8 Denoising result on kidney phantom (**a**) Original Image (**b**) Speckled noisy phantom image (**c**) SRAD (**d**) OBNLM (**e**) ADMSS (**f**) Proposed Method

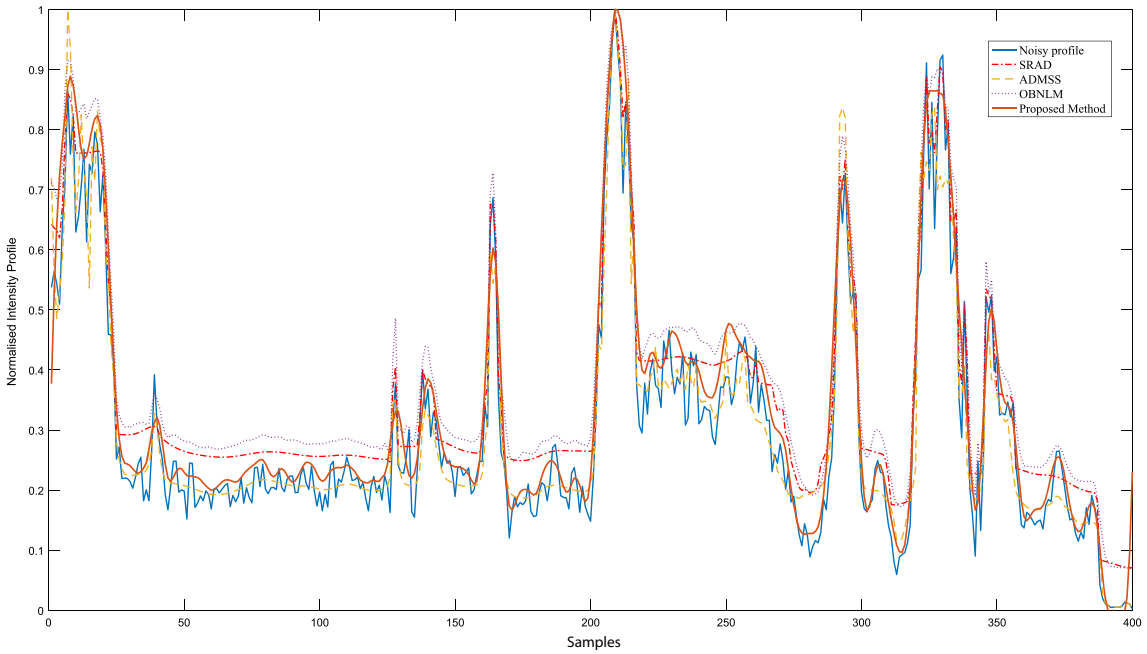

Fig. 9 Comparison of Relative Intensity profiles of denoised image and noisy image with SRAD, OBNLM, ADMSS and Proposed Method

which speckle noise is added. The denoised images shown in Fig. [8c-e] are obtained from SRAD [7], OBNLM [10], ADMSS [40] and proposed denoising method respectively. Under visual assessment, the proposed method depicts good boundaries and structural information of tissues present in the ultrasound images with a substantial reduction in speckle noise. For clear illustration, the intensity profiles are shown in Fig. 9 along with the highlighted line in the noisy image. From the intensity profiles, it is clear that the proposed method gives superior results. Experimentation also carried on the real ultrasound noisy images. Figure 10 shows the denoising results of real breast cyst image

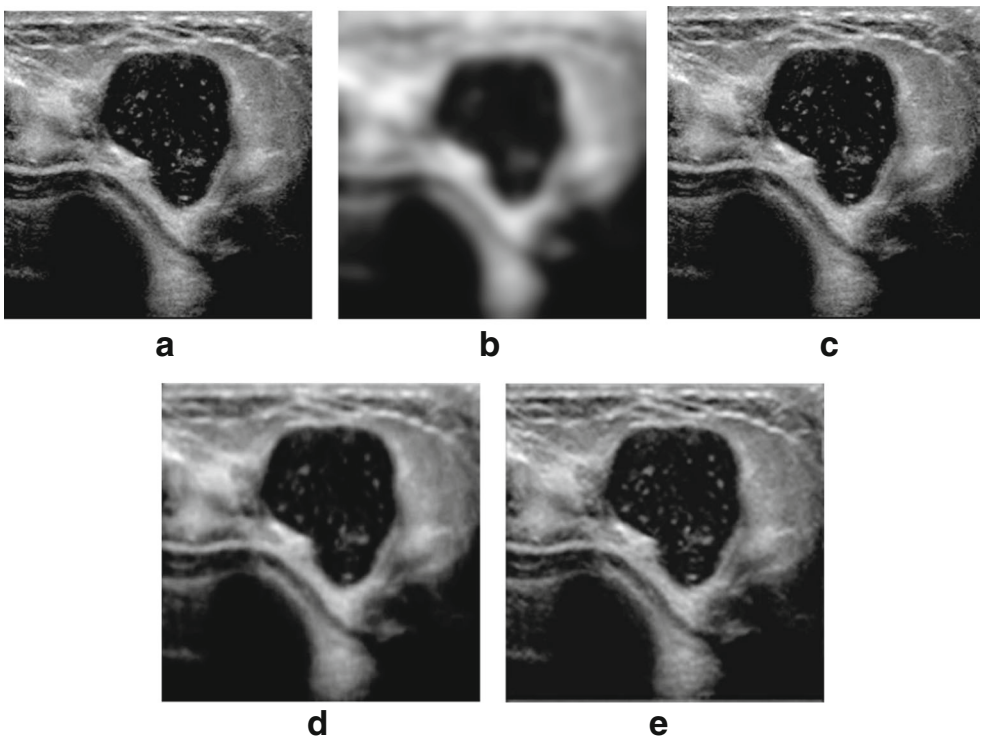

Fig. 10 Denoising result on Breast cyst philips norm image (**a**) Original Image (**b**) SRAD (**c**) OBNLM (**d**) ADMSS (**e**) Proposed Method

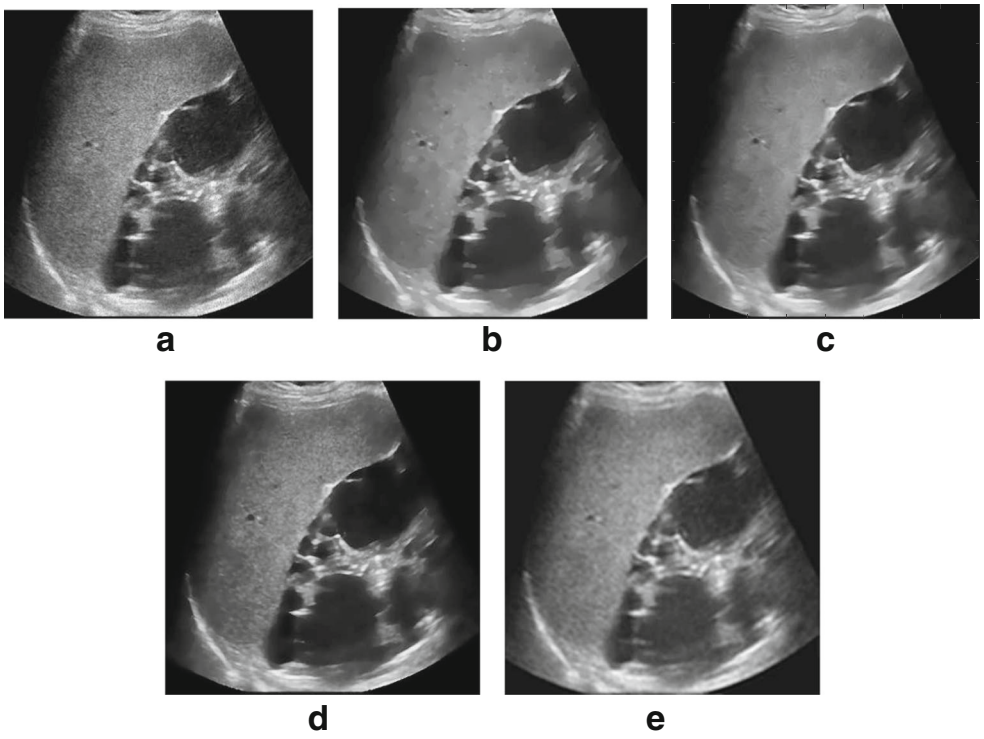

Fig. 11 Denoising result on abdomen and retro peritoneum liver database images (**a**) Original Image (**b**) SRAD (**c**) OBNLM (**d**) ADMSS (**e**) Proposed Method

obtained with all existing methods and proposed method. The proposed method comparatively reduces the speckle noise while preserving all the edges and contrast, whereas the SRAD method loses some edge information. The results of denoising on the abdomen and retro peritoneum liver database images are shown in Fig. 11. These ultrasound images were obtained from the publicly available abdomen and retro peritoneum liver and breast cyst database from "http://www.ultrasoundcases.info/". The proposed method is implemented in MATLAB R2014@a software on a computer (Intel i7 3.40 GHz CPU and 8-GB RAM). The computational time for proposed method and existing methods are given in Tables 2, 3, and 4.

To investigate the quantitative performance of the proposed method over existing methods following evaluation metrics are used.

1. *Mean Square Error (MSE)*: *MSE* measure the quality change between original image (X) and denoised image (Y). It is given by

$$MSE = \frac{1}{N^2}\sum_{i,j=1}^{N-1}(X_{ij} - Y_{ij})^2$$

2. *Signal to Noise Ratio (SNR)*: The SNR compares desired signal to the noisy signal. The higher value of ratio indicates less prominent the noise is. It is expressed in decibels (dB) as

$$SNR = 10\,log_{10}\frac{\sigma^2}{\sigma_e^2}$$

where, σ^2 and σ_e^2 are the variance of the original image and variance of the error (difference between original image with denoised image) respectively.

Table 2 Performance measures for denoising result on kideny image

Method	MSE	SNR	PSNR	SSIM	Computational Time (sec)
SRAD [7]	5.59e03	0.0394	29.39	0.0113	0.89567
OBNLM [10]	246.8	17.35	36.16	0.7934	3.82367
ADMSS [40]	76.93	21.60	38.72	0.7868	76.6941
Proposed method	58.51	22.82	39.29	0.8259	1.9297

Table 3 Performance measures for denoising result on breast cyst images

Method	MSE	SNR	PSNR	SSIM	Computational Time (sec)
SRAD [7]	6.49e03	0.0325	29.06	0.2643	0.919897
OBNLM [10]	342.32	32.19	35.45	0.5630	3.601547
ADMSS [40]	118.19	20.33	37.70	0.7663	64.07764
Proposed method	101.46	21.05	38.099	0.8773	1.987828

Table 4 Performance measures for denoising result on abdomen and retro-peritoneum liver database images

Method	MSE	SNR	PSNR	SSIM	Computational Time (sec)
SRAD [7]	6.5e03	0.00345	29.04	0.7678	1.04186
OBNLM [10]	60.06	23.49	39.2	0.7146	3.8823
ADMSS [40]	58.9	23.83	39.28	0.8470	104.944
Proposed method	57.87	24.53	39.32	0.8626	2.0935

3. *Peak Signal to Noise Ratio (PSNR)*: The *PSNR* defined as ratio between maximum power of signal and the power of the noise in the signal.

$$PSNR = 10\, log_{10} \frac{S^2}{MSE}$$

where, S is maximum intensity of the image. PSNR measures the quality of the denoised image.

4. *Structural Similarity Quality Index Measurement (SSIM)*: SSIM is used for measuring the similarity between two images. It measures the image quality.

$$SSIM = \frac{1}{M} \sum_{i=1}^{M} \frac{(2\mu_x \mu_y + C_1)(2\sigma_{xy} + C_2)}{\left(\mu_x^2 + \mu_y^2 + C1\right)\left(\sigma_x^2 + \sigma_y^2 + C_2\right)}$$

where μ_i and σ_i are the mean and standard deviation of the pixel intensities at the i^{th} location respectively and C_i is the constant. The value of *SSIM* represent the ideal structural similarity between 0-1.

Proposed Method was tested on different ultrasound images like kidney phantom, breast cyst and liver image and results are listed in Tables 2, 3 and 4 respectively. From these results, it is observed that proposed method gives better denoising results. It is also observed that edges and finer direction information efficiently preserved, which ultimately achieves good speckle noise suppression with edge preserving characteristics.

Conclusion

In this paper, a Multi-Directional Perfect Reconstruction (PR) Filter Bank design based on 2-D eigenfilter approach has been proposed. The proposed design of 2-D two-channel linear phase FIR filter banks have been used to design 2-D fan shaped, diamond shaped and checkerboard shaped type filters. The designed filter banks satisfy the perfect reconstruction criteria. Few design examples of 2-D PR filters have been demonstrated to show the effectiveness of the method, and it is observed that the proposed 2-D filters provide better symmetry, good regularity and lower energy of the error which leads to the better frequency selectivity of the filters as compared to other design methods. Moreover, the denoising algorithm used with proposed filters truly separates the clinical features and speckle noise in the ultrasound images. To quantify the performance of ultrasound image denoising, experiments have been carried on synthetic and real ultrasound images. It is observed that the performance of denoising is notably improved in terms of PSNR, SNR, MSE and SSIM evaluation metrics.

References

1. Kang, J., Lee, J. Y., and Yoo, Y., A new feature-enhanced speckle reduction method based on multiscale analysis for ultrasound b-mode imaging. *IEEE Transactions on Biomedical Engineering* 63(6):1178–1191, 2016. ISSN 0018-9294. doi:10.1109/TBME.2015.2486042.
2. Yue, Y., Croitoru, M. M., Bidani, A., Zwischenberger, J. B., and Clark, J. W., Nonlinear multiscale wavelet diffusion for speckle suppression and edge enhancement in ultrasound images. *IEEE Transactions on Medical Imaging* 25(3):297–311, 2006. ISSN 0278-0062. doi:10.1109/TMI.2005.862737.
3. Lee, J. S., Digital image enhancement and noise filtering by use of local statistics. *IEEE Transactions on Pattern Analysis and Machine Intelligence* PAMI-2(2):165–168, 1980. ISSN 0162-8828. doi:10.1109/TPAMI.1980.4766994.
4. Frost, V. S., Stiles, J. A., Shanmugan, K. S., and Holtzman, J. C., A model for radar images and its application to adaptive digital filtering of multiplicative noise. *IEEE Transactions on Pattern Analysis and Machine Intelligence* PAMI-4(2):157–166, 1982. ISSN 0162-8828. doi:10.1109/TPAMI.1982.4767223.
5. Kuan, D. T., Sawchuk, A. A., Strand, T. C., and Chavel, P., Adaptive noise smoothing filter for images with signal-dependent noise. *IEEE Transactions on Pattern Analysis and Machine Intelligence* PAMI-7(2):165–177, 1985. ISSN 0162-8828. doi:10.1109/TPAMI.1985.4767641.
6. Lopes, A., Nezry, E., Touzi, R., and Laur, H., Maximum a posteriori speckle filtering and first order texture models in sar images. In: Geoscience and Remote Sensing Symposium, 1990. IGARSS'90. 'Remote Sensing Science for the Nineties'., 10th Annual International, pp. 2409–2412, 1990. doi:10.1109/IGARSS.1990.689026.
7. Yu, Y., and Acton, S. T., Speckle reducing anisotropic diffusion. *IEEE Transactions on Image Processing* 11(11):1260–1270, 2002. ISSN 1057-7149. doi:10.1109/TIP.2002.804276.
8. Aja-Fernandez, S., and Alberola-Lopez, C., On the estimation of the coefficient of variation for anisotropic diffusion speckle filtering. *IEEE Transactions on Image Processing* 15(9):2694–2701, 2006. ISSN 1057-7149. doi:10.1109/TIP.2006.877360.
9. Krissian, K., Westin, C. F., Kikinis, R., and Vosburgh, K. G., Oriented speckle reducing anisotropic diffusion. *IEEE Transactions on Image Processing* 16(5):1412–1424, 2007. ISSN 1057-7149. doi:10.1109/TIP.2007.891803.
10. Coupe, P., Hellier, P., Kervrann, C., and Barillot, C., Nonlocal means-based speckle filtering for ultrasound images. *IEEE Transactions on Image Processing* 18(10):2221–2229, 2009. ISSN 1057-7149.
11. Pei, S.-C., Tseng, C.-C., and Yang, W.-S., Fir filter designs with linear constraints using the eigenfilter approach. *IEEE Transactions on Circuits and Systems II: Analog and Digital Signal Processing* 45(2):232–237, 1998. ISSN 1057-7130. doi:10.1109/82.661658.

12. Tkacenko, A., Vaidyanathan, P. P., and Nguyen, T., On the eigenfilter design method and its applications: A tutorial. *IEEE Transaction on Circuits and Systems* 50:497–517, 2003.
13. Vaidyanathan, P. P., and Nguyen, T., Eigenfilters: A new approach to least squares FIR filter design and applications including Nyquist filters. *IEEE Transaction on Circuits and Systems* 34(1):11–23, 1987.
14. Pei, S.-C., and Shyu, J.-J., Design of 2d fir digital filters by mcclellan transformation and least squares eigencontour mapping. *IEEE Transactions on Circuits and Systems II: Analog and Digital Signal Processing* 40(9):546–555, 1993. ISSN 1057-7130. doi:10.1109/82.257332.
15. Mersereau, R., Mecklenbrauker, W., and Quatieri, T., Mcclellan transformation for 2D filtering I-design. *IEEE Transactions on Circuits and Systems* 23(7):405–414, 1976.
16. Karam, L. J., Two-dimensional fir filter design by transformation. *IEEE Transactions on Signal Processing* 47(5):1474–1478, 1999. ISSN 1053-587X. doi:10.1109/78.757246.
17. Psarakis, E. Z., Mertzios, V. G., and Alexiou, G. P., Design of two-dimensional zero phase fir fan filters via the mcclellan transform. *IEEE Transactions on Circuits and Systems* 37(1):10–16, 1990. ISSN 0098-4094. doi:10.1109/31.45686.
18. Psarakis, E. Z., and Moustakides, G. V., Design of two-dimensional zero-phase fir filters via the generalized mcclellan transform. *IEEE Transactions on Circuits and Systems* 38(11):1355–1363, 1991. ISSN 0098-4094. doi:10.1109/31.99164.
19. Wei, D., Evans, B. L., and Bovik, A. C., Loss of perfect reconstruction in multidimensional filterbanks and wavelets designed via extended mcclellan transformations. *IEEE Signal Processing Letters* 4(10):295–297, 1997. ISSN 1070-9908. doi:10.1109/97.633773.
20. Patwardhan, P., Patil, B., and Gadre, V., Polyphase conditions and structures for 2D quincunx FIR filter banks having quadrantal or diagonal symmetries. *IEEE Transactions on Circuits and Systems II* 54(9):790–794, 2007.
21. Bolle, M., Wave digital filters for the migration of seismic data. In: 1994. ICASSP-94., 1994 IEEE International Conference on Acoustics, Speech, and Signal Processing, volume vi, pages VI/5-VI/8 vol.6, 1994. doi:10.1109/ICASSP.1994.389909.
22. Tay, D. B. H., and Kingsbury, N., Flexible design of multidimensional perfect reconstruction FIR 2-band filter-banks using transformation of variables. *IEEE Transactions on Image Processing*, 2, 1993.
23. Kovacevic, J., and Vetterli, M., Nonseparable multidimensional perfect reconstruction filter banks and wavelet bases of R^n. *IEEE Transactions on Information Theory* 38(2):533–555, 1992.
24. Patwardhan, P., and Gadre, V., Design of 2D M-th band lowpass FIR eigenfilters with symmetries. *IEEE Signal Processing Letters* 14(8):517–520, 2007.
25. Nagare, M. B., Patil, B. D., and Holambe, R. S.: Design of two-dimensional quincunx fir filter banks using eigen filter approach. IEEE International Conference on Signal and Information Processing (ICONSIP), Accepted for publication, 2016.
26. Patil, B., Patwardhan, P., and Gadre, V.: Eigenfilter approach to the design of one-dimensional and multidimensional two-channel linear phase FIR perfect reconstruction filter banks. IEEE Transactions on Circuit and Systems Vol-I, 2008.
27. Pei, S., and Shyu, J., 2D FIR eigenfilters: A least-squares approach. *IEEE Transaction on Circuits and Systems* 37:24–34, 1990.
28. Eslami, R., and Radha, H., Translation-invariant contourlet transform and its application to image denoising. *IEEE Transactions on Image Processing* 15(11):3362–3374, 2006. ISSN 1057-7149. doi:10.1109/TIP.2006.881992.
29. Lu, Y. M., and Do, M. N., Multidimensional directional filter banks and surfacelets. *IEEE Transactions on Image Processing* 16(4):918–931, 2007.
30. Vikhe, P. S., and Thool, V. R., Mass detection in mammographic images using wavelet processing and adaptive threshold technique. *Journal of Medical Systems* 40(4):82, 2016. ISSN 1573-689X. doi:10.1007/s10916-016-0435-3.
31. Olfa, M., and Nawres, K., Ultrasound image denoising using a combination of bilateral filtering and stationary wavelet transform. In: 2014 First International Image Processing, Applications and Systems Conference (IPAS), pp. 1–5, 2014. doi:10.1109/IPAS.2014.7043258.
32. Eslami, R., and Radha, H., A new family of nonredundant transforms using hybrid wavelets and directional filter banks. *IEEE Transactions on Image Processing* 16(4):1152–1167, 2007.
33. Bamberger, R. H., and Smith, M. J. T., A filter bank for the directional decomposition of images: theory and design. *IEEE Transactions on Signal Processing* 40(4):882–893, 1992. ISSN 1053-587X. doi:10.1109/78.127960.
34. Bamber, J. C., and Daft, C., Adaptive filtering for reduction of speckle in ultrasonic pulse-echo images. *Ultrasonics* 24(1):41 – 44, 1986. ISSN 0041-624X. doi:10.1016/0041-624X(86)90072-7.
35. Do, M. N., and Vetterli, M., Framing pyramids. *IEEE Transactions on Signal Processing* 51(9):2329–2342, 2003. ISSN 1053-587X. doi:10.1109/TSP.2003.815389.
36. Chang, S. G., Yu, B., and Vetterli, M., Adaptive wavelet thresholding for image denoising and compression. *IEEE Transactions on Image Processing* 9(9):1532–1546, 2000. ISSN 1057-7149. doi:10.1109/83.862633.
37. Strang, G., and Nguyen, T., *Wavelets and filter banks*. Cambridge NY: Wellesley, 1996.
38. Eslami, R., and Radha, H., Design of regular wavelets using a three-step lifting scheme. *IEEE Transactions on Signal Processing* 58(4):2088–2101, 2010.
39. Rahulkar, A. D., and Holambe, R. S., Partial iris feature extraction and recognition based on a new combined directional and rotated directional wavelet filter banks. *Neurocomputing* 81:12–23, 2012.
40. Ramos-Llordén, G., Vegas-Sánchez-Ferrero, G., Martin-Fernandez, M., Alberola-L´opez, C., and Aja-Fernández, S., Anisotropic diffusion filter with memory based on speckle statistics for ultrasound images. *IEEE Transactions on Image Processing* 24(1):345–358, 2015. ISSN 1057-7149. doi:10.1109/TIP.2014.2371244.